

# **Modular and Scalable Powertrain for Multipurpose Light Electric Vehicles**

Mehrnaz Farzam Far<sup>1</sup>, Damijan Miljavec<sup>2</sup>, Jenni Pippuri Mäkeläinen<sup>1</sup>, Mikaela Ranta<sup>1</sup>, Janne Keränen<sup>1</sup>, Jutta Kinder<sup>3</sup>, Mario Vukotić<sup>2</sup>

<sup>1</sup>*VTT Technical Research Centre of Finland, POB 1000, FI-02044 VTT, Finland, corresponding author:  
mehrnaz.farzamfar@vtt.fi*

<sup>2</sup>*University of Ljubljana, Faculty of Electrical Engineering, Trzaska 25, 1000 Ljubljana, Slovenia*

<sup>3</sup>*THIEN eDrives, GmbH, Millennium Park 11, 6890 Lustenau, Austria*

---

## **Executive Summary**

This paper presents the design of an electric powertrain for multipurpose light electric vehicles, with a focus on the motor, battery, and charging requirements. The proposed powertrain is modular and scalable in terms of the energy capacity of the battery as well as in electric motor shaft power and torque. Having such a possibility gives the flexibility to use the powertrain in different combinations for different vehicle categories, from L7 quadricycles to light M1 vehicles. The powertrain design optimization is realized from the first stages by considering the driving missions and operational patterns of the vehicle for multipurpose usage (transporting people or goods) in European urban environments.

*Keywords: charging, driving cycles, electric powertrain design, induction motor, light electric vehicle.*

---

## **1 Introduction**

Transportation is one of the fastest-growing sources of greenhouse gas emissions, accounting for 78% of the rise in emissions from 1990 to 2019 [1]. Increased use of automobiles is the main reason for this trend [1]. Although replacing all internal combustion engine (ICE) vehicles with electric vehicles (EV) is a step in the right direction, it alone is not enough to solve the problem. Additional efforts such as integrating clean energy sources, optimizing powertrains based on vehicle missions, and promoting shared vehicle usage are required to reduce emissions and achieve climate targets.

Light electric vehicles (LEVs) are particularly suitable for urban and suburban environments, where high speed and long range are not the main priorities. LEVs have lower energy consumption, higher vehicle weight-to-payload ratios, and require fewer resources for production compared to other EVs [2]. This makes them more efficient and affordable, especially for large-scale production and shared mobility scenarios.

Table 1 provides an overview of the specification of some L7e-C category EVs available in the market. All the vehicles listed in this table meet the European regulations outlined in (EU) No 168/2013 [3], which specify that L7e-C vehicles must have a maximum continuous rated power of no more than 15 kW and a maximum speed of no more than 90 km/h.

Table 1: Specifications of some L7e-C category EVs available in market

Name	Power (kW)	Max torque (Nm)	Max speed (km/h)	Voltage (V)	Battery type, capacity (kWh)	Range (km)
Honda Micro Commuter	15	N/A	80	N/A	Li-ion, N/A	96
Mahindra e-Supro van	15	90	60	72	Li-ion, 15	115
Mahindra Treo	7.5	42	55	48	Li-ion, 7.3	141
Microlino	11	89	90	N/A	Li-NMC, 14	230
Renault Twizy	13	57	80	58	Li-ion, 6.1	100
Regis Epic0 Compact	15	N/A	75	144	Li-NMC, 15.2	140
PILOT CAR, P-1000	10	102	55	48	Li-ion, 26	220
Tazzari Zero	15	150	90	80	Li-ion, 14.2	150

The design of a powertrain starts by defining various quantities such as power, torque, speed, voltage, battery capacity, and range of the vehicle. The power and torque requirements of an electric traction motor depend on the vehicle's desired performance characteristics, size, and weight. An accurate definition of the performance characteristics, and therefore reduction of the vehicle's energy consumption, requires the knowledge of the vehicle's actual driving cycles and mission. As an example, Lindh et al. [4] used an actual driving cycle of a bus route in Lappeenranta to investigate the speed and torque requirements for a heavy-duty vehicle. Based on these requirements, the authors proposed a permanent magnet traction motor design suitable for hybrid buses. However, the literature on LEV powertrain design rarely considers associated driving missions. Instead, the powertrain is first parametrized and settled, and then an ex-post performance assessment is conducted on driving cycles [5]-[8].

Different battery technologies for EVs are reviewed and compared in [9]. Lithium-ion (Li-ion) batteries are the most frequently utilized battery type in EVs due to their significantly higher energy density (Wh/kg) compared to other alternatives. The two most used Li-ion chemistries are NMC (nickel-manganese-cobalt) and LFP (lithium-iron-phosphate). NMC cells provide higher energy density and have better charging performance at low temperatures, whereas LFP cells are more affordable and have longer cycle life. The high energy density of NMC is vital for providing sufficient ranges for everyday electric driving, especially for LEV where the mass and physical dimensions of the battery have strict limitations. On contrary, the price range of LFP would better fit with LEVs. However, if the LEV is to be charged at a reasonable speed in cold climate environments, expensive and heavy thermal management systems would be required in the case of LFP batteries. Hence, optimal cell chemistry is a compromise of price, energy density, and cold climate performance. The battery capacity is determined based on various factors such as the vehicle's energy consumption, expected driving conditions, desired driving range, the weight of the vehicle, and the efficiency of the electrical motor.

The voltage levels of LEVs available in the market typically range from 48 to 80 V. The specific voltage level of an LEV is determined during the design stage, considering several factors such as the power and torque requirements of the motor, the desired range of the vehicle, and the weight and cost constraints of the battery pack. Using higher voltages in electric vehicles can be more cost-effective for energy distribution since lower currents require smaller cable cross-sections and connectors. In addition, higher voltage levels offer greater powertrain scalability towards higher categories of vehicles with superior performance characteristics, such as increased torque, power, and vehicle speed.

In this paper, we present the design of a modular and scalable electric powertrain for L7e-C category EVs with multipurpose usages (transporting people and goods), with a focus on the motor, battery, and charging requirements. The proposed electric powertrain is modular and scalable, meaning that each component can be modified according to the vehicle's mission without affecting the overall powertrain concept. This approach allows adapting the powertrain to higher classes of vehicles (e.g., M1). To ensure that the powertrain components are rightsized according to the vehicle's mission, the associated driving missions and operational patterns are considered in the design from the very first stages.

## 2 Vehicle Specifications and Operational Performance

### 2.1 Vehicle Requirements and Specifications

The first step in the design of a powertrain is to set the base specifications and requirements of the vehicle. As mentioned previously, this paper focuses on L7e light four-wheel EVs. To comply with the European regulation, the vehicle properties and specifications were selected based on the REGULATION (EU) No 168/2013 [3]: a mass in running order of up to 600 kg (without the battery and payload), a top speed of 90 km/h, and a maximum continuous power of 15 kW. The total gross weight of the vehicle is assumed to be 1200 kg (150 kg of which is the battery and 450 kg of payload). The 1-D vehicle model was described with basic parameters and their values: wheel radius  $R_w = 0.31$  m, vehicle front area  $A_v = 2.17$  m<sup>2</sup>, wind drag coefficient  $C_x = 0.3$ , tires pressure  $p_t = 3$  bar, the mass density of air  $\rho = 1.2$  kg/m<sup>3</sup>, and rolling resistance coefficient  $C_r$ , which is a function of vehicle speed, and the value varies between 0.0083 and 0.011.

Other basic properties required for the powertrain design include the vehicle's driving range, and torque and power profiles. The methodologies used to derive these properties are presented in Sub-section 2.2.

### 2.2 Range

To ensure that the powertrain components are rightsized according to the vehicle's mission, the associated driving missions and operational patterns should be considered in the design from the very first stages. For this purpose, we used a driving cycle from typical trips in a European city such as Helsinki to study the vehicle driving range, torque-speed profile, and power requirements. This driving cycle was identified as representative of a typical trip in the Helsinki region with a mix of urban and suburban driving conditions. It is worth noting that the presented driving cycle also includes the terrain shape in form of road elevation changes during the velocity profile. The speed and elevation profiles of this driving cycle are illustrated in Fig. 1.

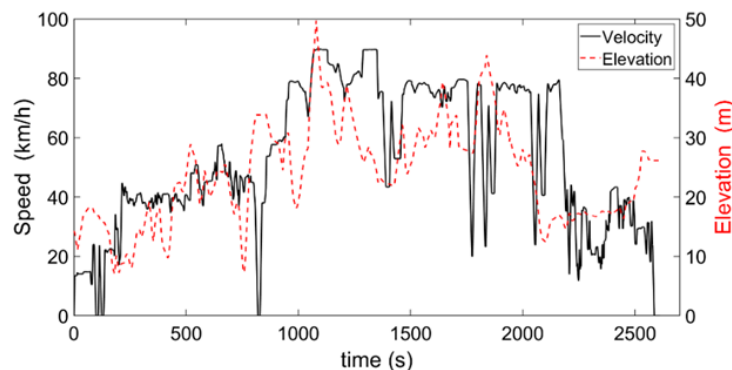


Figure 1: Speed and elevation profiles of the Helsinki region with a mix of urban and suburban driving conditions.

According to the highest allowable vehicle speed (90 km/h), wheel radius of 0.31 m (R15), and maximum electric motor rotational speed ( $10000 \text{ min}^{-1}$ ), we defined a gear ratio of 12:1 with a mean efficiency of 95%. Applying the identified Helsinki driving cycle and incorporating upper boundary conditions, we calculated the vehicle's needed torque and shaft power requirements. Figs 2 and 3 present the power and torque profiles of an electrical machine for the Helsinki driving cycle without and with considering 450 kg payload in the vehicle weight, respectively.

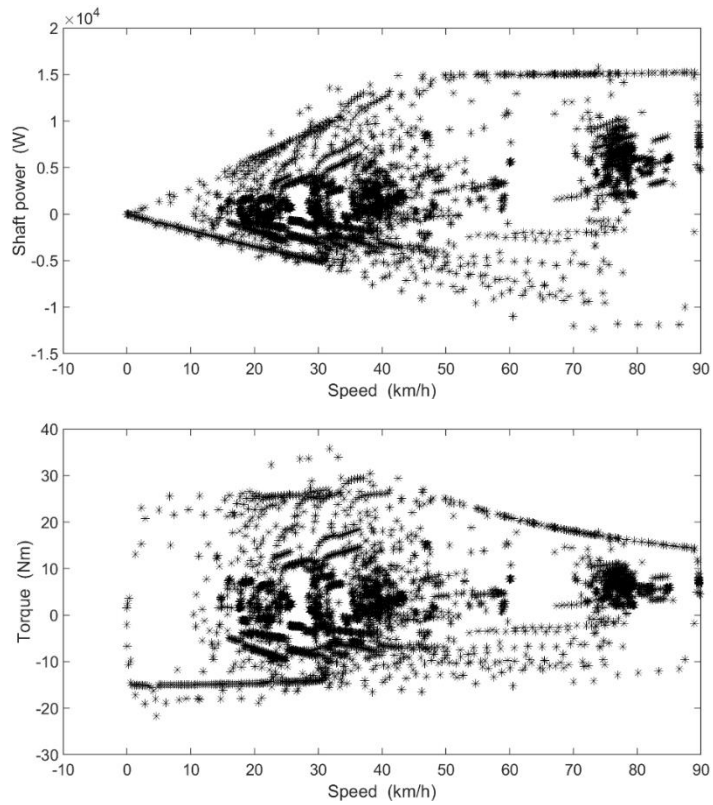


Figure 2: Power-speed (top) and torque-speed (bottom) profiles of an electrical machine for the Helsinki driving cycle with a total vehicle weight of 750 kg.

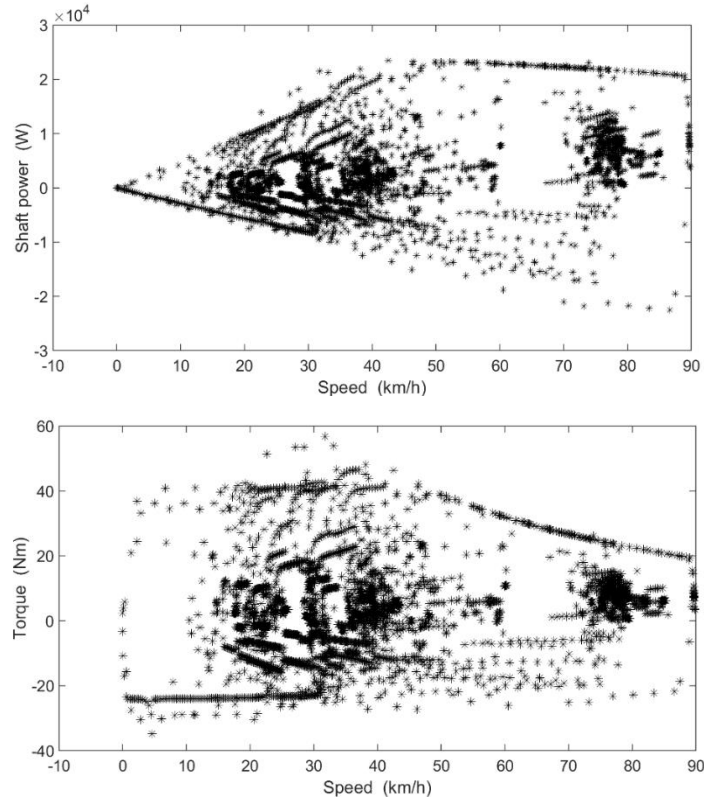


Figure 3: Power-speed (top) and torque-speed (bottom) profiles of an electrical machine for the Helsinki driving cycle with a total vehicle weight of 1200 kg (including 450 kg payload).

Further, the energy consumption at each driving point and the cumulative needed energy within one cycle were calculated. Overall energy consumed in the case of an unloaded vehicle is 2.73 kWh in one driving cycle (38.2 km) including road profile in form of elevation (Fig. 1). In the case of a fully loaded vehicle (payload 450 kg), the consumed energy is 3.56 kWh. To achieve a range of approximately 100 km and enable shorter charging times even with standard 3-phase home charging facilities, the battery must provide enough energy to allow the vehicle to complete at least three Helsinki driving cycles, covering a total distance of 114.6 km. For such distance, the electric energy consumed by the battery ranges between 8.16 kWh and 10.68 kWh. If we assume a 30% battery safety margin, the battery should have an energy capacity in the range of 15 kWh.

Based on calculated torque and power profiles (Figs. 2 and 3), the following electro-mechanical requirements were established for the design of the electrical machine:

- The electrical machine should be capable of delivering a shaft power of 15 kW in the constant power operational region, with this region extending up to a speed of 90 km/h corresponding with a motor speed of 9240  $\text{min}^{-1}$  (Fig. 2 – top figure).
- The machine should have a nominal torque of approximately 40 Nm (Fig. 2 – bottom figure) in the case of an unloaded vehicle. Meanwhile, the power and maximum torque reach up to 23 kW and 60 Nm, respectively, due to the vehicle's full payload (Fig. 3).
- The electric machine's torque-speed curve should have a corner point between 35 – 50 km/h, corresponding with a motor speed of around 3600 – 5100  $\text{min}^{-1}$ , to ensure that the torque demands remain within the region of highest efficiency for the electric machine.
- The variation of torque between 40 Nm and 60 Nm depends on the vehicle payload and the driving cycle's starting condition.

The crossroad dynamics in the form of acceleration rate will be additionally analyzed in the following section.

## 3 Design of Electric Powertrain

### 3.1 Traction Motor

Induction motors (IMs) and permanent magnet synchronous motors (PMSMs) are the most used electric traction motors in EVs. IMs are robust, reliable, and cost-effective. They are easy to control and the torque characteristics are proportional to the current. PMSMs, on the other hand, have higher efficiency, power density, and torque density than IMs. PMSMs perform better at high speeds and can produce high torque at low speeds, but they are more complex and expensive to produce due to the use of critical raw materials.

The type of traction motor chosen for an EV depends on the specific requirements. PMSMs are often used for high-performance EVs, while IMs are preferred for low-cost EVs. In this work, we chose an IM for the traction motor due to its robustness and to avoid the use of rare earth materials. The boundary conditions and requirements for designing the motor were selected for the gear ratio 12:1 as follows:

- Continuous power of 15 kW through the whole speed range (Fig. 2 – top figure) and peak power of 23 kW (Fig. 3 – top figure).
- Nominal torque of 40 Nm (Fig. 2 – bottom figure) and maximum torque of 60 Nm (Fig. 3 – bottom figure)
- Maximum torque of 70 Nm at zero speed to overcome the curb (calculated based on wheel size, vehicle mass and curb high of 15 cm).
- Nominal phase RMS voltage in the range of 125 V to 175 V, allowing lower electric currents and smaller electric power wires cross sections.
- Maximum rotational speed of the motor should be 10000  $\text{min}^{-1}$ , due to 90 km/h maximum vehicle speed limitation, wheel size, and gearbox ratio).
- Maximum motor efficiency > 92%.

To minimize the motor's size and maximize its overload operational capabilities, we selected a liquid cooling system instead of an air-cooling system. The liquid cooling system offers higher heat removal capability, especially when the vehicle is heavily loaded at lower rotational speeds.

Considering these conditions and requirements, we simulated and studied several lamination designs and selected the one that provided the desired efficiency-based speed, pole pair number, value of stator nominal current, and total nominal power. The lamination design of the proposed traction motor is presented in Fig. 4 (right). Three different axial lengths were investigated to determine the optimized length for the motor. Table 2 presents the main parameters of these three designs. The final form of the proposed induction motor with liquid cooling is shown in Fig. 4 (left).

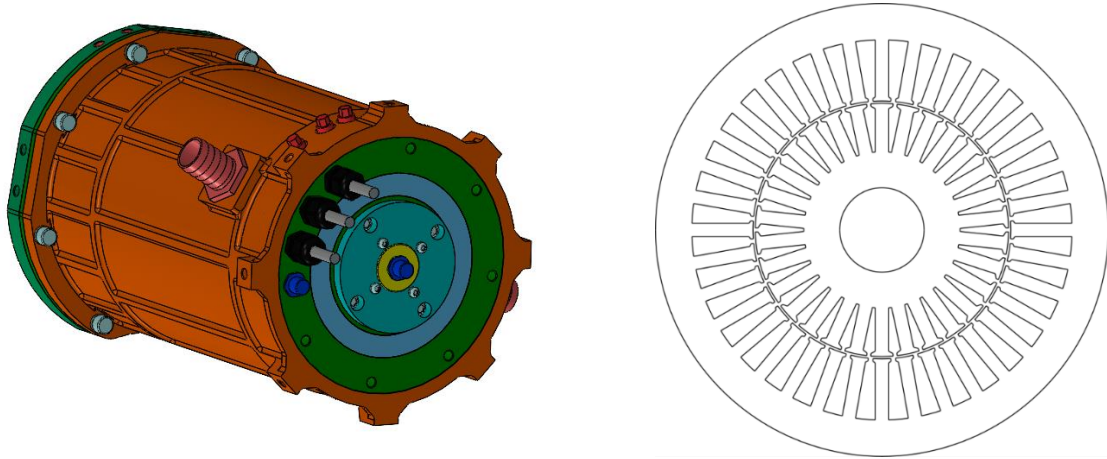


Figure 4: Design of the scalable traction motor (left) with the stator and rotor lamination (right).

Table 2: Design specifications of the proposed traction motors

Motor variant	Motor 1	Motor 2	Motor 3
Continuous power (kW)		15	
Core material	Cogent M270-35A		
Material of stator winding and rotor bars	Copper		
Number of pole pairs	2		
Number of stator slots/rotor bars	36 / 30		
Stator core outer diameter (mm)	170		
Stator core inner diameter (mm)	96.8		
Air gap width (mm)	0.4		
Shaft diameter (mm)	32		
Core length stator/rotor (mm)	200	150	100
Peak power (kW)	47.5	40.6	29.9
Base speed ( $\text{min}^{-1}$ )	4000	4380	4680
Peak torque (Nm)	127.0	97.3	66.9
Maximum efficiency (%)	94.5	93.9	92.5
Total weight (kg)	46.1	38.3	30.8

Fig. 5 presents the efficiency maps of the three motor designs, which were calculated using the 2D finite element method. The efficiency maps show the maximum achievable power values without any electric

current limitations. As can be seen from the efficiency maps, Motor 1 with the corner point at 4000 rpm has the largest efficiency area in comparison to the other motors.

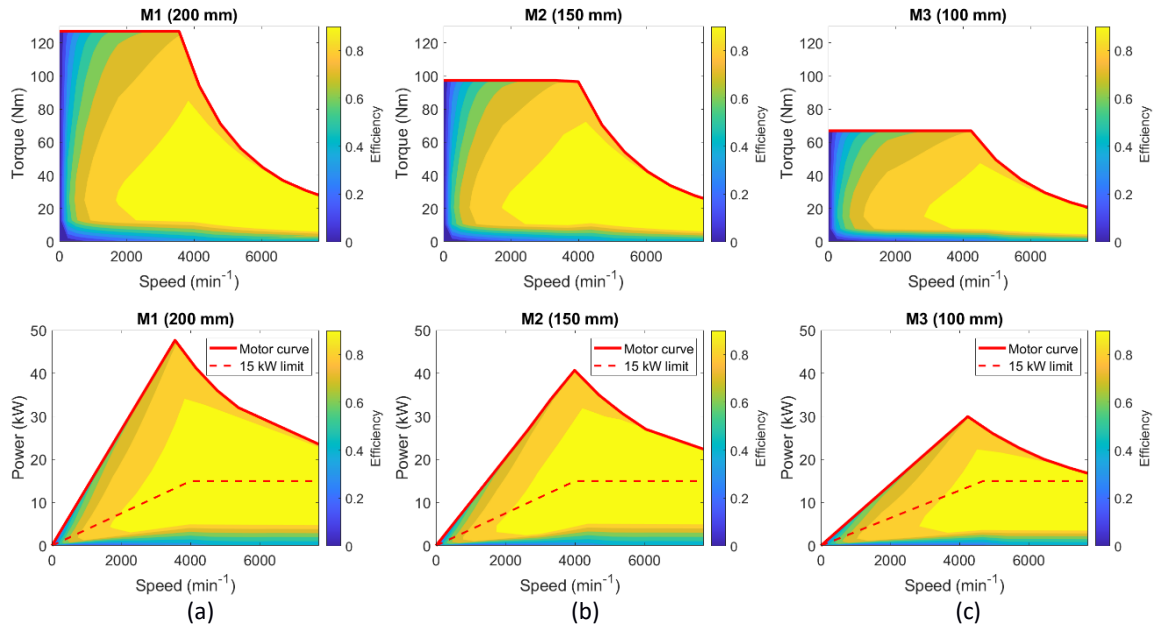


Figure 5: Efficiency maps of motor variants with different core lengths: (a) Motor 1 (200 mm), (b) Motor 2 (150 mm), and (c) Motor 3 (100 mm). Dashed lines represent power-speed profiles respecting the 15-kW continuous power limit.

### 3.2 Torque and Acceleration

The vehicle dynamics were simulated with the three motor designs. In the simulation, the resistive forces acting on the vehicle (e.g., slope, friction, air drag, etc.) and the total inertia, scaled to the electrical motor, were considered. For the gearbox and differential, the constant efficiency level of 95% was assumed. The comparison of the motors was carried out on roads with slopes ranging from 0% to 26% (maximum road slope), in terms of the maximum achievable speed and acceleration times from 0 to 40 km/h. The acceleration test results are presented in Table 3. According to these results, Motor 1 achieves the highest speeds at all slopes and outperforms the other two motors in the acceleration tests.

Table 3: Maximum achievable speed at different slopes for a fully loaded vehicle (1200 kg)

Motor	Top speed		Acceleration (0-40 km/h)	
	0% slope	26% slope	0% slope	26% slope
Motor 1	90 km/h	41.7 km/h	4.00 s	14.12 s
Motor 2	90 km/h	39.6 km/h	5.14 s	N/A
Motor 3	90 km/h	38.9 km/h	7.57 s	N/A

The torque range was established by analyzing the driving cycles, as described in Sub-section 2.2. Nevertheless, to validate the torque requirements and make any necessary adjustments, real-world urban driving cycle acceleration time was considered as well. This will further permit the adjustment of the torque characteristics of the traction motor and gearbox ratio, if needed, to fulfill the high dynamics of an EV in urban driving conditions.

The acceleration time of the urban driving condition was measured by conducting an acceleration test on a vehicle with an ICE that had similar size and weight characteristics to the vehicle under investigation. The acceleration test resulted in a time of approximately 4 seconds to reach from 0 km/h to 40 km/h. The results of this test were then utilized to define the acceleration torque requirements by inputting the data into a MATLAB software program that was designed based on the vehicle's equation of motion.

The developed MATLAB software allows for the simulation of changes in the dynamic performance of the EV powertrain, considering factors such as the torque-speed characteristic of the traction motor, the gearbox ratio, vehicle mass (1200 kg), vehicle shape (drag coefficient), wheel diameter, slope coefficient, and tire pressure. The output of the software is the calculated speed of the vehicle over time, from which the acceleration can be determined.

Fig. 6 presents the power-speed and torque-speed curves, along with the transient acceleration behavior, of all three motors at 0% slope, assuming a fully loaded vehicle with a total mass of 1200 kg. According to the results, the vehicle with Motor 1 fulfills the acceleration requirements from 0 to 40 km/h in 4 s and therefore is chosen as the traction motor of the proposed vehicle.

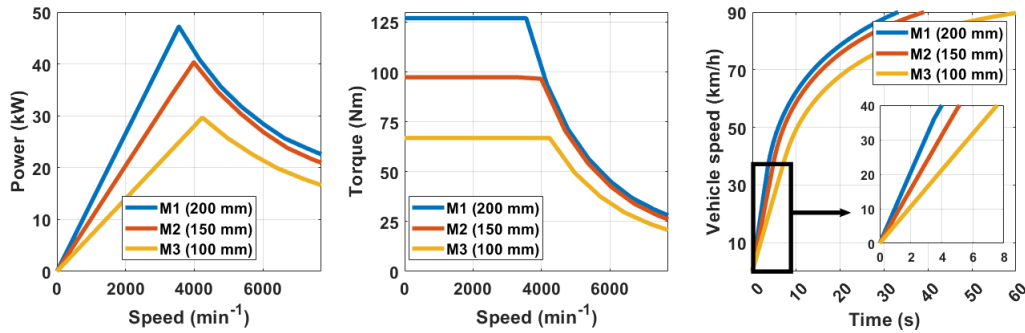


Figure 6: Influence of the power-speed (left) and torque-speed curves (middle) on the vehicle acceleration (right).

### 3.3 Battery and Frequency Inverter

Based on the upper-defined nominal phase RMS voltage level, the maximum allowable battery voltage may range from 340 V to 475 V. Another voltage limit was set by the off-the-shelf frequency inverter needed to drive the designed traction motor. We decided to use SEVCON Gen4Size8 frequency inverter [10] with a maximum voltage limit of 400 V. To achieve the maximum voltage level of 400 V, we use 95 Li-ion NMC battery cells from KOKAM (model: SLPB100216216H [11]) connected in series, each having a capacity of 40 Ah. This battery stack delivers a maximum energy of 15.8 kWh. When using cells with an average voltage of 3.7 V, the battery capacity is reduced to 14 kWh. The proposed battery assembly provides sufficient energy to fulfill the defined range of needed battery energy.

The battery designed for the vehicle has integrated BMS, contactors, fuses, DC/DC converter (400V/12 V, 1.2 kW), and air-cooling ventilators in the battery box (Fig. 7). This battery box design features an energy storage system with 14 kWh of energy capacity, fulfilling all requirements regarding voltage, vehicle range, overload capability, fast charging, and safety concerns (battery structural integrity). Moreover, the battery was built modularly, so its energy capacity can be scaled up to 25 kWh, for example, for the M1 vehicle type, just by substituting the battery cells with the ones that have a higher 60 Ah capacity, such as KOKAM Model: KCL216060EN1[12].



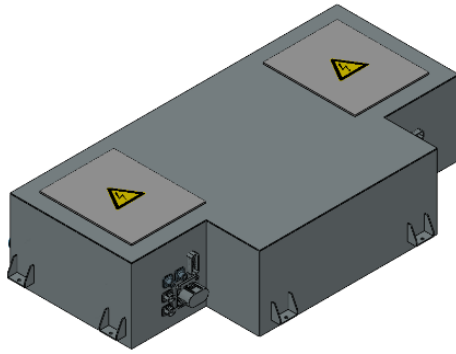


Figure 7: Modular battery for different vehicle classes (L7 to M1).

## 4 Charging Requirements

A detailed analysis of its utilization was conducted to determine the required power of the charging system. In this work, vehicle utilization is referred to as duty cycles and encompasses the trips that the vehicle is expected to make during the day. The duty cycles are presented as schedule-format descriptions of the driven route origins and destinations, non-driving related activities (such as cargo loading and unloading), and breaks from all activities when the vehicle is not occupied. The cycle profiles can be generated via mesoscopic simulations such as activity-based transport modeling (ABTM) [13]. We implemented the duty cycles into an in-house microscopic simulation tool [14] to study the charging requirements of the vehicle while considering the driving cycles, vehicle dynamics, and charging module. In the simulation, it was assumed that a fleet of about 28000 vehicles with a utility rate of 50% was distributed around the Capital Region of Helsinki (i.e., Helsinki, Espoo, Vantaa, and Kauniainen), providing a shared fleet for 24/7 transportation (e.g., people during the day and goods at night).

Fig. 8 (left) shows the simulated daily distance driven by each vehicle in the fleet. As shown in this figure, the average distance exceeds 200 km, and some vehicles travel over 300 km per day. Fig. 8 (right) displays the maximum available charging time between each trip, assuming that charging is feasible at all locations where the vehicles park.

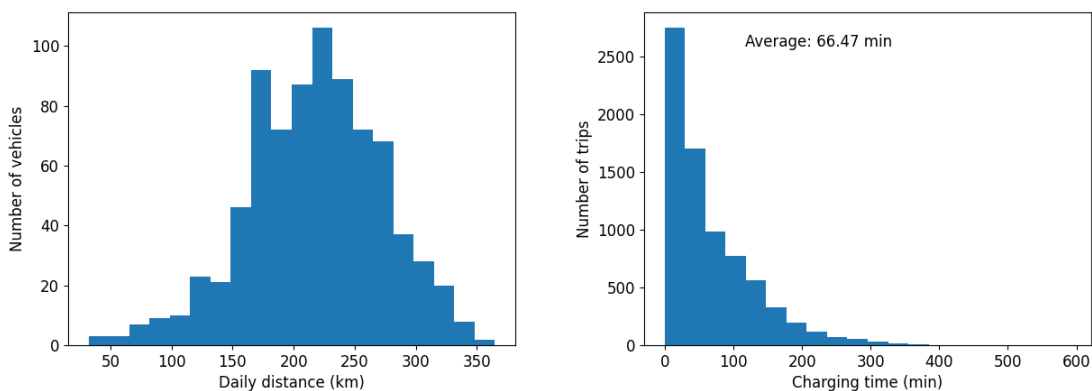


Figure 8: Distribution of the simulated daily distance of each vehicle (left) and maximum available charging time between the trips (right).

To gain an understanding of the vehicle operation in a more realistic situation where charging is not always possible, the parking locations of the vehicles from the initial simulations were analyzed and the 100 most often used locations were set to be equipped with a charger, while other parking locations were left without

charging facilities. Out of the 100 charging locations, 20% were equipped with fast 7 kW chargers and the rest with slower 3.7 kW chargers.

Table 4 summarizes the results of two charging scenarios: one with charging available at all parking locations, and the other with charging available at only 100 locations. In the first scenario, all scheduled trips were fulfilled without the battery state of charge (SOC) dropping below 35%. In the second scenario, some vehicles could not complete their trips due to high daily distances. Nevertheless, on average 92% of the daily target distance was covered, and the issues were mostly related to the very last trip of the day. It is worth noting that the simulations did not consider certain driver behaviors, such as selecting a vehicle with a higher SOC or choosing a parking spot with a charger instead of one without. Accounting for these factors would likely increase the likelihood of completing all the trips. Therefore, a 7 kW was chosen as the maximum charging power of the vehicle. With such power, the battery will be charged from zero to 100% SOC in a bit more than 2 hours.

Table 4: Summary of simulated duty cycle with two charging scenarios

Charging scenario	Completed daily distance (mean (min–max))	Trips/day (mean (min–max))	Completed distance vs. target
Slow charging (3.7 kW) available at all parking locations	217.6 km (32.1–364.7) km	10.5 (1–20)	100%
Slow charging (3.7 kW) at 80 locations, fast charging (7 kW) at 20 locations	196.6 km (32.1–326.6) km	9.8 (1–17)	92.4%

## 5 Conclusions

This paper presents the design of an electric powertrain for multipurpose light electric vehicles, with a focus on the motor, battery, and charging requirements. The first step of the design involved studying a driving cycle from a typical European city such as Helsinki, to derive the vehicle's driving range, torque-speed profile, and power requirements. This ensures that the proposed design is optimized according to the vehicle's driving missions and operational patterns. Three models for the traction motor were proposed based on torque and power profiles, and the vehicle dynamics for each motor were studied. The most efficient motor was found to meet the vehicle dynamics criterion of accelerating from 0 to 40 km/h in 4 seconds. The battery capacity was estimated based on the driving range. The maximum charging power of the vehicle was set to 7 kW after a detailed analysis of the vehicle's expected utilization throughout the day.

## Acknowledgments

This work was fully supported by the EU REFLECTIVE project, funded by the European Union's Horizon 2020 research and innovation program under grant agreement No. 101006747.

## References

- [1] M. Ge, J. Friedrich and L. Vigna, "4 Charts Explain Greenhouse Gas Emissions by Countries and Sectors," 6 February 2020. [Online]. Available: <https://www.wri.org/insights/4-charts-explain-greenhouse-gas-emissions-countries-and-sectors#>. [Accessed 24 October 2022].
- [2] S. Ehrenberger, I. Dasgupta, M. Brost, L. Gebhardt and R. Seiffert, "Potentials of Light Electric Vehicles for Climate Protection by Substituting Passenger Car Trips," *World Electric Vehicle Journal*, vol. 13, no. 10, 2022.
- [3] Consolidated text: Regulation (EU) No 168/2013 of the European Parliament and of the Council of 15 January 2013 on the approval and market surveillance of two- or three-wheel vehicles and quadricycles (Text with EEA relevance), 2020.

- [4] P. Lindh, M. Gerami Tehrani, T. Lindh, J. H. Montonen, J. Pyrhönen, J. T. Sopanen, M. Niemelä, Y. Alexandrova, P. Immonen, L. Aarniovuori and M. Polikarpova, "Multidisciplinary Design of a Permanent-Magnet Traction Motor for a Hybrid Bus Taking the Load Cycle into Account," *IEEE Transactions on Industrial Electronics*, vol. 63, no. 6, pp. 3397-3408, 2016.
- [5] V. Ruuskanen, J. Nerg, A. Parviainen, M. Rilla and J. Pyrhönen, "Design and Drive-cycle Based Analysis of Direct-driven Permanent Magnet Synchronous Machine for a Small Urban Use Electric Vehicle," in *16th European Conference on Power Electronics and Applications*, Lappeenranta, 2014.
- [6] V. Ruuskanen, J. Nerg, J. Pyrhönen, R. S. and R. Kennel, "Drive Cycle Analysis of a Permanent-Magnet Traction Motor Based on Magnetostatic Finite-Element Analysis," *IEEE Transactions on Vehicular Technology*, vol. 64, no. 3, pp. 1249-1254, 2015.
- [7] A. Łebkowski, "Light Electric Vehicle Powertrain Analysis," *Scientific Journal of Silesian University of Technology. Series Transport*, vol. 94, pp. 123-137, 2017.
- [8] M. Chirca, M. A. Dranca, S. Breban and C. A. Oprea, "PMSM Evaluation for Electric Drive Train for L6e Light Electric Vehicles," in *International Conference and Exposition on Electrical And Power Engineering (EPE)*, Iasi, 2020.
- [9] M. Houache, C.-H. Yim, Z. Karkar and Y. Abu-Lebdeh, "On the Current and Future Outlook of Battery Chemistries for Electric Vehicles—Mini Review," *Batteries*, vol. 8, no. 7, 2022.
- [10] BorgWarner, "AC Motor Controller Gen4 Size 8," BorgWarner, [Online]. Available: [https://cdn.borgwarner.com/docs/default-source/default-document-library/gen4-size-8.pdf?sfvrsn=4b2b5a3d\\_7](https://cdn.borgwarner.com/docs/default-source/default-document-library/gen4-size-8.pdf?sfvrsn=4b2b5a3d_7). [Accessed 20 March 2023].
- [11] Kokam, "Superior Lithium ion Battery," Kokam, 21 May 2021. [Online]. Available: [https://kokam.com/uploaded/filebox/7/cell\\_brochure.pdf](https://kokam.com/uploaded/filebox/7/cell_brochure.pdf). [Accessed 20 March 2023].
- [12] Kokam, "Kokam Li-ion Cell," Kokam, 2021. [Online]. Available: <https://kokam.com/en/product/cell/lithium-ion-battery>. [Accessed 20 March 2023].
- [13] Z. A. Needell and J. E. Trancik, "Efficiently Simulating Personal Vehicle Energy Consumption in Mesoscopic Transport Models," *Transportation Research Record*, vol. 2672, no. 25, pp. 163-173, 2018.
- [14] J. Anttila, Y. Todorov, M. Ranta and Pihlatie, "System-Level Validation of an Electric Bus Fleet Simulator," in *IEEE Vehicle Power and Propulsion Conference (VPPC)*, Hanoi, 2019.

## Presenter Biography



Mehrnaz Farzam Far received her M.Sc. (Tech.) and D.Sc. (Tech.) degrees in electrical engineering from the Department of Electrical Engineering and Automation at Aalto University, Finland in 2014 and 2019, respectively. She joined VTT Technical Research Centre of Finland in 2019, where she works as a senior scientist in the Electrical Powertrains and Storage team. She has experience with electric drives, numerical analysis and design of electrical machines, and model order reduction methods. She is currently working on the design of charging systems for electric vehicles and their charging infrastructure and standardization.